

Polarisation effects of the dynamical Stark effect of excitons in quantum wells

This article has been downloaded from IOPscience. Please scroll down to see the full text article.

1990 J. Phys.: Condens. Matter 2 5979

(<http://iopscience.iop.org/0953-8984/2/27/005>)

View [the table of contents for this issue](#), or go to the [journal homepage](#) for more

Download details:

IP Address: 171.66.16.103

The article was downloaded on 11/05/2010 at 06:00

Please note that [terms and conditions apply](#).

Polarisation effects of the dynamical Stark effect of excitons in quantum wells

J Schlösser†, A Stahl† and I Balslev‡

† Institut für Theoretische Physik, Rheinisch-Westfälische Technische Hochschule, Aachen, D-5100 Aachen, Federal Republic of Germany

‡ Fysisk Institut, Odense Universitet, Odense, Denmark

Received 12 September 1989, in final form 3 January 1990

Abstract. We study the polarisation properties of the dynamical Stark effect of excitons in semiconductor quantum wells. We start from a four-band density matrix theory involving the heavy- and light-hole band and the two lowest conduction subbands. The set of equations of motion contains the dynamics relevant for both Fröhlich-type experiments (pumping with a carbon dioxide laser) and the case of pumping a few exciton rydbergs below the exciton line. We perform the relevant projections based on excitonic eigenstates and study the resulting 'few-level' systems. From this we calculate the change in the susceptibility tensor with respect to a weak probe beam caused by a pump beam with specified polarisation and frequency.

1. Introduction

An interesting non-linear optical effect is the so-called dynamical Stark effect of excitons in semiconductors, i.e. the modification of the excitonic absorption caused by a strong pump beam in the transparent spectral region. Fröhlich *et al* [1, 2] studied experimentally the case of an infrared pump beam in resonance with a transition between the exciton state considered and a secondary exciton state. In contrast with this 'resonant' Stark effect, Mysyrowicz *et al* [3] and von Lehmen *et al* [4] studied the 'non-resonant' case in which the pump frequency is of the order of one or a few exciton rydbergs below the exciton line considered.

Fröhlich *et al* [1, 2] used a three-level model for explaining the resonant effect. As for the non-resonant effect the theories reported range from simple dressed-atom approaches [5] and two-level models [6] to elaborate Hartree–Fock schemes [7–10]. Most of the theoretical work reported so far does not consider the full valence band structure, and so the polarisation properties of the Stark effect are not discussed in any detail. Exceptions are the papers by Combescot [11] and Joffre *et al* [12] who in a perturbative treatment derive relevant selection rules for the non-resonant effect.

In the present paper we shall calculate the polarisation properties associated with the different types of dynamical Stark effect. As in most experiments mentioned above, we regard the exciton dynamics in a multi-quantum well (MQW). The starting point will be the electron–hole density matrix theory [13, 14] extended to include the necessary number of valence and conduction band sublevels as specified in section 2. In section 3 we treat the resonant (Fröhlich-type) effect in a MQW, while the non-resonant effect will

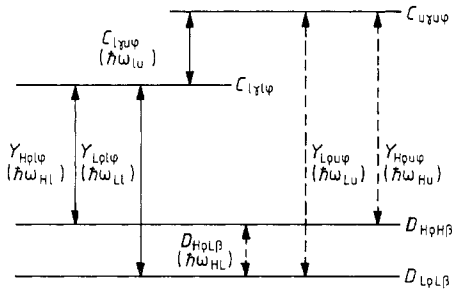


Figure 1. Level diagram. The $C_{ly\psi\varphi}$, $C_{uy\psi\varphi}$, $D_{L\rho L\beta}$ and $D_{H\rho H\beta}$ are level occupancies. The transition densities are $Y_{K\rho l\varphi}$, $Y_{K\rho u\varphi}$ ($K = H, L$) and $C_{ly\psi\varphi}$, $D_{H\rho L\beta}$. The allowed transitions are indicated by full arrows, and the forbidden transitions by broken arrows.

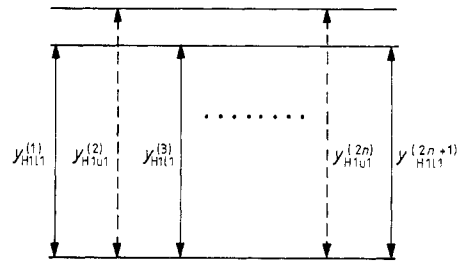


Figure 2. Iteration procedure for $y_{H11}^{(2n-1)}$. The full arrows indicate transition densities that do contribute to polarisation, and the broken arrows those that do not contribute. No occupancies contribute and the infrared transitions are not active.

be studied in section 4. In order to simplify the algebra we neglect throughout the Fock-type exchange integrals in the equations of motion for the density matrices. By neglecting these, the analysis is restricted to cases where the pump frequency is not too close to the exciton resonance.

It turns out that in Fröhlich-type experiments [1, 2] with an infrared pump the dominant non-linearity is provided by the pump field acting on the exciton envelope. In contrast with this the decisive non-linearity in a Mysyrowicz-type experiment [3, 4] is due to the Pauli blocking terms in the equations of motion. This distinction also manifests itself in the corresponding selection rules.

2. Four-band density matrix theory

Let us assume that a set of Bloch functions are given as a result of a band-structure calculation for a GaAs–Al_xGa_{1-x}As MQW. For simplicity, we use the band structure in a diagonal approximation and the states in the envelope-function approximation for a single well. According to the experimental situations [2, 3, 4, 12] we consider only the lowest conduction sub-bands for which the indices u and l are used for upper ($n = 2$) and lower ($n = 1$), respectively. The valence bands considered are the $n = 1$ sub-band of the heavy-hole (index, H) and the $n = 1$ sub-band of the light hole (index, L), the corresponding energy gaps will be $\hbar\omega_{HI}$, $\hbar\omega_{HU}$, etc. We treat the exciton in the two-dimensional limit and use r as the relative coordinate in the plane of the well. We apply the long-wave limit for the electric field E and may therefore drop the centre-of-mass coordinate. The Fock-type exchange integrals [13, 14] will be neglected.

When setting up the four-band model we use Y for electron–hole matrices, D for hole–hole matrices and C for electron–electron matrices (figure 1). The equations of motion then take on the form

$$\begin{aligned}
 -i\hbar\dot{Y}_{H\rho l\varphi} + \hbar\Omega_{HI}Y_{H\rho l\varphi} = E \cdot \left(\bar{M}_{\varphi\rho}^H \delta(r) \frac{1}{w} - \sum_{\lambda} \bar{M}_{\lambda\rho}^H C_{\lambda l\varphi} \right. \\
 \left. - \sum_{\kappa} \bar{M}_{\varphi\kappa}^H D_{H\kappa H\rho} - \sum_{\kappa} \bar{M}_{\varphi\kappa}^L D_{H\rho L\kappa}^* + \bar{m}_0 Y_{H\rho u\varphi} \right) \tag{1a}
 \end{aligned}$$

$$-i\hbar\dot{Y}_{L\rho l\varphi} + \hbar\Omega_{Ll}Y_{L\rho l\varphi} = E \cdot \left(\tilde{M}_{\varphi\rho}^L \delta(\mathbf{r}) \frac{1}{w} - \sum_{\lambda} \tilde{M}_{\lambda\rho}^L C_{l\lambda l\varphi} - \sum_{\kappa} \tilde{M}_{\varphi\kappa}^L D_{L\kappa L\rho} - \sum_{\kappa} \tilde{M}_{\varphi\kappa}^H D_{H\kappa L\rho} + \tilde{m}_0 Y_{L\rho u\varphi} \right) \quad (1b)$$

$$-i\hbar\dot{Y}_{H\rho u\varphi} + \hbar\Omega_{Hu}Y_{H\rho u\varphi} = E \cdot \left(\tilde{m}_0 Y_{H\rho l\varphi} - \sum_{\lambda} \tilde{M}_{\lambda\rho}^H C_{l\lambda u\varphi} \right) \quad (1c)$$

$$-i\hbar\dot{Y}_{L\rho u\varphi} + \hbar\Omega_{Lu}Y_{L\rho u\varphi} = E \cdot \left(\tilde{m}_0 Y_{L\rho l\varphi} - \sum_{\lambda} \tilde{M}_{\lambda\rho}^L C_{l\lambda u\varphi} \right) \quad (1d)$$

$$-i\hbar\dot{C}_{l\gamma u\varphi} + \hbar\Omega_{lu}C_{l\gamma u\varphi} = E \cdot \left(\tilde{m}_0 (C_{l\gamma l\varphi} - C_{u\gamma u\varphi}) - \sum_{\kappa} \tilde{M}_{\gamma\kappa}^{H*} Y_{H\kappa u\varphi} - \sum_{\kappa} \tilde{M}_{\gamma\kappa}^{L*} Y_{L\kappa u\varphi} \right) \quad (1e)$$

$$-i\hbar\dot{D}_{H\rho l\beta} + \hbar\Omega_{HL}D_{H\rho l\beta} = E \cdot \left(\sum_{\lambda} (\tilde{M}_{\lambda\beta}^L Y_{H\rho l\lambda}^* - \tilde{M}_{\lambda\rho}^{H*} Y_{L\beta l\lambda}) \right) \quad (1f)$$

$$-i\hbar\dot{C}_{l\gamma l\varphi} = E \cdot \left(\sum_{\kappa} (\tilde{M}_{\varphi\kappa}^H Y_{H\kappa l\gamma}^* - \tilde{M}_{\gamma\kappa}^{H*} Y_{H\kappa l\varphi}) + \sum_{\kappa} (\tilde{M}_{\varphi\kappa}^L Y_{L\kappa l\gamma}^* - \tilde{M}_{\gamma\kappa}^{L*} Y_{L\kappa l\varphi}) + \tilde{m}_0 (C_{l\gamma u\varphi} - C_{l\varphi u\gamma}^*) \right) \quad (1g)$$

$$-i\hbar\dot{C}_{u\gamma u\varphi} = E \cdot [\tilde{m}_0 (C_{l\varphi u\gamma}^* - C_{l\gamma u\varphi})] \quad (1h)$$

$$-i\hbar\dot{D}_{H\rho H\beta} = E \cdot \left(\sum_{\lambda} (\tilde{M}_{\lambda\beta}^H Y_{H\rho l\lambda}^* - \tilde{M}_{\lambda\rho}^{H*} Y_{H\beta l\lambda}) \right) \quad (1i)$$

$$-i\hbar\dot{D}_{L\rho L\beta} = E \cdot \left(\sum_{\lambda} (\tilde{M}_{\lambda\beta}^L Y_{L\rho l\lambda}^* - \tilde{M}_{\lambda\rho}^{L*} Y_{L\beta l\lambda}) \right). \quad (1j)$$

The propagation operators are

$$\hbar\Omega_{Kl} = \hbar\omega_{Kl} - (\hbar^2/2\mu_{iK})[\partial^2/\partial r^2 + (1/r)(\partial/\partial r)] - e^2/4\pi\epsilon\epsilon_0 r + e\mathbf{E} \cdot \mathbf{r} \quad (2a)$$

$$\hbar\Omega_{Ku} = \hbar\omega_{Ku} - (\hbar^2/2\mu_{iK})[\partial^2/\partial r^2 + (1/r)(\partial/\partial r)] - e^2/4\pi\epsilon\epsilon_0 r + e\mathbf{E} \cdot \mathbf{r} \quad (2b)$$

$$\hbar\Omega_{lu} = \hbar\omega_{lu} + e\mathbf{E} \cdot \mathbf{r} \quad (2c)$$

$$\hbar\Omega_{HL} = \hbar\omega_{HL} - e\mathbf{E} \cdot \mathbf{r}. \quad (2d)$$

The index K is equivalent to H or L. The Greek indices specify the total angular momentum quantum numbers of the $\mathbf{k} = \mathbf{0}$ Bloch functions and take the values 1 and 2 corresponding to the Kramers degeneracies. The z axis is normal to the well plane and also the quantisation direction for the angular momentum. The transition dipoles $\tilde{M}_{\varphi\rho}^K$ describe the optical coupling between the lower conduction sub-band and the valence band K. \tilde{m}_0 denotes the transition dipole between the conduction bands 1 ($n = 1$) and u ($n = 2$). \tilde{m}_0 is oriented along z and its magnitude is of the order of $20e \text{ \AA}$ for a well width w of the order of 100 \AA . Evaluating the quantities $\tilde{M}_{\varphi\rho}^K$ using group theoretical methods, one arrives at

$$\tilde{M}_{\varphi\rho}^K = \tilde{M}_0 \langle u_{\varphi}^1 | \hat{p} | u_{\rho}^K \rangle \quad (3a)$$

$$\tilde{M}_{11}^H = \tilde{M}_0 \frac{1}{\sqrt{2}} \begin{bmatrix} 1 \\ i \\ 0 \end{bmatrix} \quad \tilde{M}_{22}^H = \tilde{M}_0 \frac{1}{\sqrt{2}} \begin{bmatrix} 1 \\ -i \\ 0 \end{bmatrix} \quad (3b)$$

$$\tilde{M}_{12}^H = \mathbf{0} \quad \tilde{M}_{21}^H = \mathbf{0}$$

$$\tilde{M}_{11}^L = \tilde{M}_0 \frac{-\sqrt{2}}{\sqrt{3}} e_z \quad \tilde{M}_{22}^L = \tilde{M}_0 \frac{-\sqrt{2}}{\sqrt{3}} e_z$$

$$\tilde{M}_{12}^L = \tilde{M}_0 \frac{-1}{\sqrt{6}} \begin{bmatrix} 1 \\ -i \\ 0 \end{bmatrix} \quad \tilde{M}_{21}^L = \tilde{M}_0 \frac{1}{\sqrt{6}} \begin{bmatrix} 1 \\ i \\ 0 \end{bmatrix}. \quad (3c)$$

Note that transitions from the heavy-hole band to the l conduction sub-band are forbidden in the case of polarisation along z.

The polarisation reads

$$\begin{aligned} P = 2 \operatorname{Re} \left[\tilde{M}_0^* \begin{bmatrix} 1 \\ -i \\ 0 \end{bmatrix} \left(\frac{1}{\sqrt{2}} Y_{H111} + \frac{1}{\sqrt{6}} Y_{L112} \right) + \tilde{M}_0^* \begin{bmatrix} 1 \\ i \\ 0 \end{bmatrix} \left(\frac{1}{\sqrt{2}} Y_{H212} - \frac{1}{\sqrt{6}} Y_{L211} \right) \right. \\ \left. - \tilde{M}_0^* \frac{\sqrt{2}}{\sqrt{3}} \mathbf{e}_z (Y_{L111} + Y_{L212}) + \tilde{m}_0 \mathbf{e}_z (C_{11u1} + C_{12u2}) \right]_{r=0}. \end{aligned} \quad (4)$$

Following ideas formulated in [15–17] we may expand the density matrices in terms of stationary exciton state wavefunctions $\Psi_K^m(\mathbf{r})$:

$$Y_{K\rho l\varphi} = \sum_m y_{K\rho l\varphi}^m(t) \Psi_K^m(\mathbf{r}) \quad (5a)$$

$$Y_{K\rho u\varphi} = \sum_m y_{K\rho u\varphi}^m(t) \Psi_K^m(\mathbf{r}) \quad (5b)$$

$$C_{l\gamma u\varphi} = \sum_m c_{l\gamma u\varphi}^m(t) \Psi_K^m(\mathbf{r}) \quad (5c)$$

$$D_{H\rho L\beta} = \sum_m d_{H\rho L\beta}^m(t) \Psi_K^m(\mathbf{r}) \quad (5d)$$

$$C_{l\gamma l\varphi} = \sum_m c_{l\gamma l\varphi}^m(t) \Psi_K^m(\mathbf{r}) \quad (5e)$$

$$C_{u\gamma u\varphi} = \sum_m c_{u\gamma u\varphi}^m(t) \Psi_K^m(\mathbf{r}) \quad (5f)$$

$$D_{K\rho K\beta} = \sum_m d_{K\rho K\beta}^m(t) \Psi_K^m(\mathbf{r}). \quad (5g)$$

The summation runs over bound states as well as unbound states of the exciton continuum. Note that in (5c)–(5f) it is left open whether the basis functions $\Psi_K^m(\mathbf{r})$ are those with heavy holes or light holes (compare also the remark following equation (15)).

3. Fröhlich-type Stark effects

In our calculation of the resonant Stark effect we assume a pump-and-probe situation as described in [2]. The strong pump beam is resonant with the lu transition, ω_{lu} is much smaller than the gap frequencies ω_{Kl} and ω_{Ku} and the frequency ω of the weak probe is close to ω_{Hl} and ω_{Ll} . We first consider in this section the effect of the z component of the pump field. The influence of the xy components will be discussed in the last part of the section.

From resonance arguments alone, it can be seen that, with infrared pumping, only the first four of equations (1a)–(1j) are active. In other words, one can neglect both DC and oscillating components of the electron–electron and hole–hole density matrices. Furthermore, only the lowest 1s term in the expansion (5a)–(5g) is relevant (unless the pump is resonant with a 1s–np transition within an exciton series). Let us denote these lowest coefficients as $y_{K\rho l\varphi}(t)$ and $y_{K\rho u\varphi}(t)$. The relevant equations of motion then become

$$-i\hbar\dot{y}_{K\rho l\varphi} + \hbar\tilde{\omega}_{Kl}^{1s} y_{K\rho l\varphi} = \mathbf{E} \cdot [\tilde{M}_{\varphi\rho}^K \Psi_K^{1s*}(0)(1/w) + \tilde{m}_0 y_{K\rho u\varphi}] \quad (6a)$$

$$-i\hbar\dot{y}_{K\rho u\varphi} + \hbar\tilde{\omega}_{Ku}^{1s} y_{K\rho u\varphi} = \mathbf{E} \cdot \tilde{m}_0 y_{K\rho l\varphi} \quad (6b)$$

where the excitonic energies with superscript 1s are

$$\hbar\tilde{\omega}_{Kl}^{1s} = \hbar\omega_{Kl} - 4\hbar\omega_{Ry} - i\hbar\Gamma_{2Kl} \quad (7a)$$

$$\hbar\tilde{\omega}_{Ku}^{1s} = \hbar\omega_{Ku} - 4\hbar\omega_{Ry} - i\hbar\Gamma_{2Ku}. \quad (7b)$$

We have introduced phenomenological dephasing rates Γ_{2Kl} and Γ_{2Ku} . $4\hbar\omega_{Ry}$ is the binding energy of the lowest two-dimensional exciton state. Note that, since the electron–electron and the hole–hole density matrices are not involved, the exchange integrals [13, 14] also vanish. So the dominant contributions to the Fröhlich-type Stark effect are not influenced by exchange-type non-linearities.

As reported previously [18, 19], the equations of type (6a) and (6b) can be solved iteratively to infinite order in E_z^{pu} and first order in E^{pr} . For example for the components y_{Hlll} and y_{Hlul} we find that

$$\begin{aligned} -i\hbar\dot{y}_{Hlll}^{(1)} + \hbar\tilde{\omega}_{Hl}^{1s}y_{Hlll}^{(1)} &= \tilde{M}_0(1/\sqrt{2})(E_x^{pr} + iE_y^{pr})\Psi_H^{1s*}(0)(1/w) \\ &\vdots \\ -i\hbar\dot{y}_{Hlul}^{(2n)} + \hbar\tilde{\omega}_{Hu}^{1s}y_{Hlul}^{(2n)} &= \tilde{m}_0E_z^{pu}y_{Hlll}^{(2n-1)} \\ -i\hbar\dot{y}_{Hlll}^{(2n+1)} + \hbar\tilde{\omega}_{Hl}^{1s}y_{Hlll}^{(2n+1)} &= \tilde{m}_0E_z^{pu}y_{Hlul}^{(2n)}. \end{aligned} \tag{8}$$

Figure 2 illustrates this iterative procedure. The Fourier transform of $y_{Hlll}^{(2n+1)}$, assuming a monochromatic pump, forms a geometric series and can be summed analytically [18].

A more attractive procedure for solving (6a) and (6b) is based on Fourier transformation. We obtain the following integral equation for the Fourier transform $\tilde{y}_{K\rho l\varphi}(\omega)$ of $y_{K\rho l\varphi}(t)$:

$$\begin{aligned} \tilde{y}_{K\rho l\varphi}(\omega) = \frac{1}{\hbar(\tilde{\omega}_{Kl}^{1s} - \omega)} &\left(\Psi_K^{1s*}(0) \frac{1}{w} \tilde{M}_{\varphi\rho}^K \cdot \tilde{E}^{pr}(\omega) \right. \\ &\left. + \frac{|\tilde{m}_0|^2}{(2\pi)^2} \int d\eta_1 d\eta_2 \frac{\tilde{E}_z^{pu}(\omega - \eta_1)\tilde{E}_z^{pu}(\eta_1 - \eta_2)}{\hbar(\tilde{\omega}_{Ku}^{1s} - \eta_1)} \tilde{y}_{K\rho l\varphi}(\eta_2) \right) \end{aligned} \tag{9}$$

which in the present case of monochromatic pump has the solution

$$\begin{aligned} \tilde{y}_{K\rho l\varphi}(\omega) = [\Psi_K^{1s*}(0)/w] &\{ \hbar(\tilde{\omega}_{Ku}^{1s} - \omega_{pu} - \omega) / [\hbar^2(\tilde{\omega}_{Kl}^{1s} - \omega)(\tilde{\omega}_{Ku}^{1s} - \omega_{pu} - \omega) \\ &- |\tilde{m}_0\tilde{E}_z^{pu}(\omega_{pu})|^2] \} \tilde{M}_{\varphi\rho}^K \cdot \tilde{E}^{pr}(\omega) \end{aligned} \tag{10}$$

as also obtained by a summation of the geometrical series in the above iterative procedure [18].

Equations (6a) and (6b) show that the previously reported simplification of the band edge equations (BEEs) leading to a three-level system [16] can be carried out further because the active parts of equations (1a)–(1j) are only the $y_{K\rho l\varphi}$ and $y_{K\rho u\varphi}$ inter-band transitions (see figure 2). Surprisingly, the inter-sub-band density matrices for lu transitions, which are in resonance with the infrared pump beam, are zero (within the framework of the approximations applied).

The result for Fourier transform $\tilde{P}(\omega)$ of the polarisation (4) reads

$$\begin{aligned} \tilde{P}(\omega) = \varepsilon_0 \left[\sum_K \frac{|\Psi_K^{1s}(0)|^2}{w\varepsilon_0} \left(\sum_{\varphi,\rho} \tilde{M}_{\varphi\rho}^{K*} \otimes \tilde{M}_{\varphi\rho}^K \right) \right. \\ \left. \times \frac{\hbar(\tilde{\omega}_{Ku}^{1s} - \omega_{pu} - \omega)}{\hbar^2(\tilde{\omega}_{Kl}^{1s} - \omega)(\tilde{\omega}_{Ku}^{1s} - \omega_{pu} - \omega) - |\tilde{m}_0\tilde{E}_z^{pu}(\omega_{pu})|^2} \right] \cdot \tilde{E}^{pr}(\omega) \\ = \varepsilon_0 \tilde{\chi}(\omega) \tilde{E}^{pr}(\omega) \end{aligned} \tag{11}$$

with

$$\sum_{\rho,\varphi} \tilde{M}_{\varphi\rho}^{H*} \otimes \tilde{M}_{\varphi\rho}^H = |\tilde{M}_0|^2 \begin{pmatrix} 1 & 0 & 0 \\ 0 & 1 & 0 \\ 0 & 0 & 0 \end{pmatrix} \quad \sum_{\rho,\varphi} \tilde{M}_{\varphi\rho}^{L*} \otimes \tilde{M}_{\varphi\rho}^L = \frac{|\tilde{M}_0|^2}{3} \begin{pmatrix} 1 & 0 & 0 \\ 0 & 1 & 0 \\ 0 & 0 & 4 \end{pmatrix}. \tag{12}$$

Wille [20] used an expression which is the scalar form of (11). It is seen that the

Fröhlich-type Stark effect is independent of the polarisation of the probe beam as long as \mathbf{E}^{pr} is in the plane of the well. This could also be seen from fundamental symmetry arguments.

It is important to note that the above contribution to the dynamical Stark effect belongs to a pump beam fully polarised along z . There is in addition a non-resonant Fröhlich-type contribution for an xy -polarised pump field. This originates from transitions to excitons with p_x, p_y symmetry.

In the case of infrared pumping with xy polarisation, one has to consider the non-linearity caused by the $\mathbf{E} \cdot \mathbf{r}$ term in the electron-hole propagators (2a). This term activates the contributions $y_{K\rho\varphi}^m$ in the expansion (5a) where m stands for x and y components of two-dimensional excitonic p states. The dominant term is the $2p$ contribution. The relevant set of equations is

$$-i\hbar\dot{y}_{K\rho\varphi} + \hbar\bar{\omega}_{Kl}^{1s}y_{K\rho\varphi} = \mathbf{E} \cdot \left(\tilde{\mathbf{M}}_{\varphi\rho}^K \frac{\Psi_K^{1s*}(0)}{w} + \tilde{m}_0 y_{K\rho\varphi} \right) + \tilde{m}_1 \sum_m E_m y_{K\rho\varphi}^m \quad (13a)$$

$$-i\hbar\dot{y}_{K\rho\varphi}^m + \hbar\bar{\omega}_{Kl}^{2p}y_{K\rho\varphi}^m = \mathbf{E}_m \cdot \tilde{m}_1 y_{K\rho\varphi} \quad m = x, y \quad (13b)$$

$$-i\hbar\dot{y}_{K\rho\varphi} + \hbar\bar{\omega}_{Ku}^{1s}y_{K\rho\varphi} = \mathbf{E} \cdot \tilde{m}_0 y_{K\rho\varphi}. \quad (13c)$$

The $1s$ -to- $2p$ dipole matrix element \tilde{m}_1 appearing in the response equations (13b) is of the order e times an exciton Bohr radius, which is more than ten times larger than \tilde{M}_0 . Furthermore the pump frequency in the Fröhlich experiment is much closer to the frequency of the $1s$ -to- $2p$ transition than to the gap, and so the Pauli blocking can be neglected. The non-resonant Fröhlich-type Stark effect via $1s$ -to- $2p$ transitions is likely to explain the spectra observed by Fröhlich *et al* using pump polarisation in the plane of the well.

Retaining only $2p$ states in the sum of (13a) and employing a Fourier transformation, one obtains

$$\begin{aligned} \tilde{\mathbf{P}}(\omega) = \varepsilon_0 \left[\sum_K \frac{|\Psi_K^{1s}(0)|^2}{w\varepsilon_0} \left(\sum_{\varphi,\rho} \tilde{\mathbf{M}}_{\varphi\rho}^{K*} \otimes \tilde{\mathbf{M}}_{\varphi\rho}^K \right) \left(\hbar(\bar{\omega}_{Kl}^{1s} - \omega) \right. \right. \\ \left. \left. - \frac{|\tilde{m}_0 \tilde{\mathbf{E}}_z^{\text{pu}}(\omega_{\text{pu}})|^2}{\hbar(\bar{\omega}_{Ku}^{1s} - \omega_{\text{pu}} - \omega)} - \frac{2|\tilde{m}_1 \tilde{\mathbf{E}}_t^{\text{pu}}(\omega_{\text{pu}})|^2}{\hbar(\bar{\omega}_{Kl}^{2p} - \omega) - \hbar\omega_{\text{pu}}^2/(\bar{\omega}_{Kl}^{2p} - \omega)} \right)^{-1} \right] \cdot \tilde{\mathbf{E}}^{\text{pr}}(\omega) \\ = \varepsilon_0 \tilde{\chi}(\omega) \tilde{\mathbf{E}}^{\text{pr}}(\omega) \end{aligned} \quad (14)$$

where $\tilde{\mathbf{E}}_t^{\text{pu}} \perp \mathbf{e}_z$ and $\bar{\omega}_{Kl}^{2p}$ is the frequency of the lowest two-dimensional p states minus the phenomenological damping term $i\Gamma_{2Kl}^{2p}$.

Figure 3 compares the resonant and the 'non-resonant' Fröhlich-type Stark effects according to experimental situations [2, 20]. The arrows give the positions of the $1s$ resonances in the unpumped spectra. The agreement with experiments is satisfactory, because the fitted value of \tilde{m}_1 is $60e \text{ \AA}$. This value is close to e times the Bohr radius of the $2d$ exciton.

Note that no optical Kerr effect is expected in the case of infrared non-resonant pumping.

4. The non-resonant Stark effect

In this section we shall discuss the situation in which the pump is not in resonance with any transitions either from the ground state or from the exciton level considered. As in

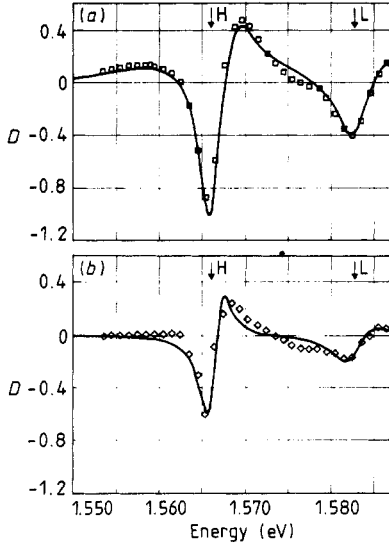


Figure 3. Differential absorption change D of a GaAs–Al $_x$ Ga $_{1-x}$ As MQW of thickness $w = 83.5 \text{ \AA}$ calculated from (14): (a) with the pump along z and (b) with the pump perpendicular to z . \square , \diamond , scanned experimental data from [2] (figure 2(a)). The arrows denote the positions of 1s resonances in the unpumped spectra. We used the following parameter set for both cases: $\hbar\omega_{\text{H1}}^{\text{L}} = 1.566 \text{ eV}$, $\hbar\omega_{\text{L1}}^{\text{L}} = 1.5827 \text{ eV}$, $\hbar\omega_{\text{K1}}^{\text{L}} = \hbar\omega_{\text{K1}}^{\text{L}} + 110.3 \text{ meV}$, $\hbar\omega_{\text{H1}}^{\text{H}} = 1.5718 \text{ eV}$, $\hbar\omega_{\text{L1}}^{\text{H}} = 1.5885 \text{ eV}$, $\hbar\Gamma_{2\text{H1}} = \hbar\Gamma_{2\text{H1}}^{\text{H}} = 1.6 \text{ meV}$, $\hbar\Gamma_{2\text{L1}} = \hbar\Gamma_{2\text{L1}}^{\text{H}} = 2.9 \text{ meV}$, $|\tilde{m}_0 \tilde{E}_2^{\text{pu}}(\omega_{\text{pu}})| = 5.9 \text{ meV}$, $|\tilde{m}_1 \tilde{E}_1^{\text{pu}}(\omega_{\text{pu}})| = 33.4 \text{ meV}$ and therefore $\tilde{m}_1 = 6\tilde{m}_0$, $\tilde{m}_0 = 15e \text{ \AA}$.

[12] we assume the polarisation of both pump and probe beams to be in the plane of the well. The detuning is assumed to be larger than a few rydbergs because the neglected exchange integrals become important for smaller values of the detuning. As the z component of the electric field is absent, the relevant equations of motion are those of a three-band system involving the valence bands H, L and the lower conduction band l. In this section we therefore drop the indices u, l. The relevant equations are

$$-i\hbar\dot{Y}_{\text{H}\rho\varphi} + \hbar\Omega_{\text{H}} Y_{\text{H}\rho\varphi} = E \cdot \left(\tilde{M}_{\varphi\rho}^{\text{H}} \delta(r) \frac{1}{w} - \sum_{\lambda} \tilde{M}_{\lambda\rho}^{\text{H}} C_{\lambda\varphi} - \sum_{\kappa} \tilde{M}_{\varphi\kappa}^{\text{H}} D_{\text{H}\kappa\text{H}\rho} - \sum_{\kappa} \tilde{M}_{\varphi\kappa}^{\text{L}} D_{\text{H}\rho\text{L}\kappa}^* \right) \quad (15a)$$

$$-i\hbar\dot{Y}_{\text{L}\rho\varphi} + \hbar\Omega_{\text{L}} Y_{\text{L}\rho\varphi} = E \cdot \left(\tilde{M}_{\varphi\rho}^{\text{L}} \delta(r) \frac{1}{w} - \sum_{\lambda} \tilde{M}_{\lambda\rho}^{\text{L}} C_{\lambda\varphi} - \sum_{\kappa} \tilde{M}_{\varphi\kappa}^{\text{L}} D_{\text{L}\kappa\text{L}\rho} - \sum_{\kappa} \tilde{M}_{\varphi\kappa}^{\text{H}} D_{\text{H}\kappa\text{L}\rho} \right) \quad (15b)$$

$$-i\hbar\dot{D}_{\text{H}\rho\text{L}\beta} + \hbar\Omega_{\text{HL}} D_{\text{H}\rho\text{L}\beta} = E \cdot \left(\sum_{\lambda} (\tilde{M}_{\lambda\beta}^{\text{L}} Y_{\text{H}\rho\lambda}^* - \tilde{M}_{\lambda\rho}^{\text{H}*} Y_{\text{L}\beta\lambda}) \right) \quad (15c)$$

$$-i\hbar\dot{C}_{\gamma\varphi} = E \cdot \left(\sum_{\kappa} (\tilde{M}_{\varphi\kappa}^{\text{H}} Y_{\text{H}\kappa\gamma}^* - \tilde{M}_{\gamma\kappa}^{\text{H}*} Y_{\text{H}\kappa\varphi}) + \sum_{\kappa} (\tilde{M}_{\varphi\kappa}^{\text{L}} Y_{\text{L}\kappa\gamma}^* - \tilde{M}_{\gamma\kappa}^{\text{L}*} Y_{\text{L}\kappa\varphi}) \right) \quad (15d)$$

$$-i\hbar\dot{D}_{\text{H}\rho\text{H}\beta} = E \cdot \left(\sum_{\lambda} (\tilde{M}_{\lambda\beta}^{\text{H}} Y_{\text{H}\rho\lambda}^* - \tilde{M}_{\lambda\rho}^{\text{H}*} Y_{\text{H}\beta\lambda}) \right) \quad (15e)$$

$$-i\hbar\dot{D}_{\text{L}\rho\text{L}\beta} = E \cdot \left(\sum_{\lambda} (\tilde{M}_{\lambda\beta}^{\text{L}} Y_{\text{L}\rho\lambda}^* - \tilde{M}_{\lambda\rho}^{\text{L}*} Y_{\text{L}\beta\lambda}) \right). \quad (15f)$$

As [11] we neglect the different reduced mass of excitons derived from the two valence bands. We consider a pump beam in the same spectral range as the exciton resonance. Then the dominant non-linear effects are due to band filling in which case we may neglect the $E \cdot r$ contributions in the propagation operators Ω and project the

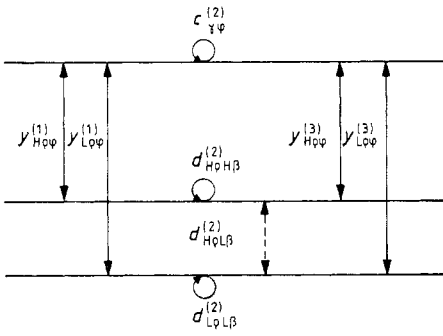


Figure 4. Third-order iteration procedure. y , c and d are the time-dependent expansion coefficients according to the 1s projection. The full arrows indicate transition densities that do contribute to polarisation, and the broken arrows those that do not contribute. Occupancies contribute in second order.

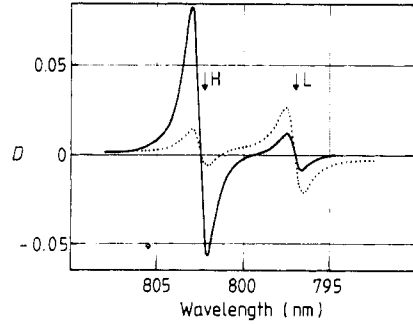


Figure 5. Differential absorption change $-D$ of a GaAs-Al_xGa_{1-x}As MQW of thickness $w = 100 \text{ \AA}$ calculated from (18a)–(18d); the unit nm is used according to [12]. The coupling is induced by a '+' pump. Theoretical spectra are shown for a '+' (—) and a '-' (····) probe polarisation. We used the following parameters: $\Gamma_{1c} = \Gamma_{1K} = \Gamma_{2HL} = 0.3 \text{ meV}/\hbar$, $\Gamma_{2K} = 1.52 \text{ meV}/\hbar$. $\hbar\omega_{H\beta}^{1s} = 1.548 \text{ eV}$ and $\hbar\omega_{L\beta}^{1s} = 1.559 \text{ eV}$. The arrows denote the positions of the 1s resonances in the unpumped spectra. $\hbar\omega_{HL} = 11 \text{ meV}$ and $\hbar\omega_{pu} = 1.456 \text{ eV}$. The pump intensity is 100 MW cm^{-2} .

BEEs to the exciton level considered, i.e. the 1s exciton. Unlike the situation in section 3 it is hardly possible to calculate analytically the response to infinite order in the pump field. An illustration of the first steps of an iteration procedure is shown in figure 4. These steps are relevant for calculating the third-order susceptibility $\chi^{(3)}$. This quantity is obtained by inserting the Fourier solutions of the projected equations of motion into (4).

In relation to the experimental situation it is convenient to give results in terms of the change $\Delta\chi$ of the first-order susceptibility with respect to the probe caused by a spectrally narrow pump beam. Since the third-order polarisation is given by

$$\tilde{P}_i^{(3)}(\omega) = \varepsilon_0 \sum_{j,k,l} \chi_{ijkl}^{(3)}(\omega_{pu}, -\omega_{pu}, \omega) \tilde{E}_j^{\text{pu}}(\omega_{pu}) \tilde{E}_k^{\text{pu}*}(\omega_{pu}) \tilde{E}_l^{\text{pr}}(\omega) \quad (16)$$

we calculate the quantity

$$\Delta\chi_{ii}(\omega) = \sum_{j,k} \chi_{ijkl}^{(3)}(\omega_{pu}, -\omega_{pu}, \omega) \tilde{E}_j^{\text{pu}}(\omega_{pu}) \tilde{E}_k^{\text{pu}*}(\omega_{pu}). \quad (17)$$

The tilde denotes Fourier transform. Retaining only the most resonant terms one arrives at the following formulae:

$$\begin{aligned} \Delta\chi_{xx}(\omega) = & \sum_{\mathbf{K}} a_{\mathbf{K}} \{ (|\tilde{E}_x^{\text{pu}}|^2 + |\tilde{E}_y^{\text{pu}}|^2) [g_{\mathbf{K}}^1(\omega) + b_{\mathbf{K}} g_{\mathbf{K}}^2(\omega)] \\ & + b_{\mathbf{K}} (|\tilde{E}_x^{\text{pu}}|^2 - |\tilde{E}_y^{\text{pu}}|^2) g_{\mathbf{K}}^3(\omega) \} \end{aligned} \quad (18a)$$

$$\begin{aligned} \Delta\chi_{yy}(\omega) = & \sum_{\mathbf{K}} a_{\mathbf{K}} \{ (|\tilde{E}_x^{\text{pu}}|^2 + |\tilde{E}_y^{\text{pu}}|^2) [g_{\mathbf{K}}^1(\omega) + b_{\mathbf{K}} g_{\mathbf{K}}^2(\omega)] \\ & - b_{\mathbf{K}} (|\tilde{E}_x^{\text{pu}}|^2 - |\tilde{E}_y^{\text{pu}}|^2) g_{\mathbf{K}}^3(\omega) \} \end{aligned} \quad (18b)$$

$$\Delta\chi_{xy}(\omega) = \sum_{\mathbf{K}} a_{\mathbf{K}} \{2i \operatorname{Im}(\tilde{E}_x^{\text{pu}} \tilde{E}_y^{\text{pu}*}) [g_{\mathbf{K}}^1(\omega) - b_{\mathbf{K}} g_{\mathbf{K}}^2(\omega)] + b_{\mathbf{K}} 2 \operatorname{Re}(\tilde{E}_x^{\text{pu}} \tilde{E}_y^{\text{pu}*}) g_{\mathbf{K}}^3(\omega)\} \quad (18c)$$

$$\Delta\chi_{yx}(\omega) = \sum_{\mathbf{K}} a_{\mathbf{K}} \{-2i \operatorname{Im}(\tilde{E}_x^{\text{pu}} \tilde{E}_y^{\text{pu}*}) [g_{\mathbf{K}}^1(\omega) - b_{\mathbf{K}} g_{\mathbf{K}}^2(\omega)] + b_{\mathbf{K}} 2 \operatorname{Re}(\tilde{E}_x^{\text{pu}} \tilde{E}_y^{\text{pu}*}) g_{\mathbf{K}}^3(\omega)\} \quad (18d)$$

where

$$a_{\mathbf{K}} = [|\Psi_{\mathbf{K}}^{1s}(0)|^2 / 2W\varepsilon_0 \hbar^3] |\tilde{M}_0 / \sqrt{j_{\mathbf{K}}}|^4 \quad j_{\text{H}} = 2 \quad j_{\text{L}} = 6$$

$$b_{\text{H}} = \frac{1}{3} \quad b_{\text{L}} = 3$$

and

$$g_{\mathbf{K}}^1(\omega) = [-1/(\tilde{\omega}_{\mathbf{K}} - \omega)] \{ [1/(\omega - \omega_{\text{pu}} + i\Gamma_{1\mathbf{K}}) + 1/(\omega - \omega_{\text{pu}} + i\Gamma_{1c})] \times [1/(\tilde{\omega}_{\mathbf{K}} - \omega) - 1/(\tilde{\omega}_{\mathbf{K}}^* - \omega_{\text{pu}})] + 2\Gamma_{2\mathbf{K}}(1/\Gamma_{1\mathbf{K}} + 1/\Gamma_{1c}) \times \{1/[(\omega_{\mathbf{K}} - \omega_{\text{pu}})^2 + \Gamma_{2\mathbf{K}}^2]\} \} \quad (19a)$$

$$g_{\text{H}}^2(\omega) = [-1/(\tilde{\omega}_{\text{H}} - \omega)] \{ [1/(\tilde{\omega}_{\text{HL}}^* + \omega - \omega_{\text{pu}})] [1/(\tilde{\omega}_{\text{H}} - \omega) - 1/(\tilde{\omega}_{\text{L}}^* - \omega_{\text{pu}})] + 2\Gamma_{2\text{L}}(1/\Gamma_{1c}) \{1/[(\omega_{\text{L}} - \omega_{\text{pu}})^2 + \Gamma_{2\text{L}}^2]\} \} \quad (19b)$$

$$g_{\text{L}}^2(\omega) = [-1/(\tilde{\omega}_{\text{L}} - \omega)] \{ [-1/(\tilde{\omega}_{\text{HL}} - \omega + \omega_{\text{pu}})] [1/(\tilde{\omega}_{\text{L}} - \omega) - 1/(\tilde{\omega}_{\text{H}}^* - \omega_{\text{pu}})] + 2\Gamma_{2\text{H}}(1/\Gamma_{1c}) \{1/[(\omega_{\text{H}} - \omega_{\text{pu}})^2 + \Gamma_{2\text{H}}^2]\} \} \quad (19c)$$

$$g_{\text{H}}^3(\omega) = [-1/(\tilde{\omega}_{\text{H}} - \omega)] \{ [1/(i\Gamma_{1c} + \omega - \omega_{\text{pu}})] [1/(\tilde{\omega}_{\text{L}} - \omega) - 1/(\tilde{\omega}_{\text{L}}^* - \omega_{\text{pu}})] + 2\Gamma_{2\text{L}}(1/\tilde{\omega}_{\text{HL}}^*) \{1/[(\omega_{\text{L}} - \omega_{\text{pu}})^2 + \Gamma_{2\text{L}}^2]\} \} \quad (19d)$$

$$g_{\text{L}}^3(\omega) = [-1/(\tilde{\omega}_{\text{L}} - \omega)] \{ [1/(i\Gamma_{1c} + \omega - \omega_{\text{pu}})] [1/(\tilde{\omega}_{\text{H}} - \omega) - 1/(\tilde{\omega}_{\text{H}}^* - \omega_{\text{pu}})] + 2\Gamma_{2\text{H}}(1/\tilde{\omega}_{\text{HL}}) \{1/[(\omega_{\text{H}} - \omega_{\text{pu}})^2 + \Gamma_{2\text{H}}^2]\} \}. \quad (19e)$$

We have introduced the following damping constants:

(i) dephasing rates in the transition frequencies

$$\tilde{\omega}_{\text{H}} := \omega_{\text{H}}^{1s} - i\Gamma_{2\text{H}} \quad \tilde{\omega}_{\text{L}} := \omega_{\text{L}}^{1s} - i\Gamma_{2\text{L}} \quad \tilde{\omega}_{\text{HL}} := \omega_{\text{HL}} - i\Gamma_{2\text{HL}} \quad (20a)$$

(ii) T_1 -like relaxation constants for the gapless transitions

$$\Gamma_{1c}, \Gamma_{1\text{H}}, \Gamma_{1\text{L}}. \quad (20b)$$

The terms in equations (19a)–(19e) with prefactors $\Gamma_{2\mathbf{K}}$ ($\mathbf{K} \equiv \text{H}, \text{L}$) are due to the dephasing of the pairs created by the pump. These terms can be neglected if the pump pulse is short and/or the detuning is large. Furthermore, one can safely neglect $\Gamma_{1\mathbf{K}}, \Gamma_{1c}, \Gamma_{2\text{HL}}$ compared with $\omega - \omega_{\text{pu}}$. This leads to the following simplified expressions:

$$g_{\mathbf{K}}^1(\omega) = [-1/(\tilde{\omega}_{\mathbf{K}} - \omega)] [2/(\omega - \omega_{\text{pu}})] [1/(\tilde{\omega}_{\mathbf{K}} - \omega) - 1/(\tilde{\omega}_{\mathbf{K}}^* - \omega_{\text{pu}})] \quad (21a)$$

$$g_{\text{H}}^2(\omega) = [-1/(\tilde{\omega}_{\text{H}} - \omega)] [1/(\omega - \omega_{\text{pu}} + \omega_{\text{HL}})] [1/(\tilde{\omega}_{\text{H}} - \omega) - 1/(\tilde{\omega}_{\text{L}}^* - \omega_{\text{pu}})] \quad (21b)$$

$$g_{\text{L}}^2(\omega) = [-1/(\tilde{\omega}_{\text{L}} - \omega)] [1/(\omega - \omega_{\text{pu}} - \omega_{\text{HL}})] [1/(\tilde{\omega}_{\text{L}} - \omega) - 1/(\tilde{\omega}_{\text{H}}^* - \omega_{\text{pu}})] \quad (21c)$$

$$g_{\text{H}}^3(\omega) = [-1/(\tilde{\omega}_{\text{H}} - \omega)] [1/(\omega - \omega_{\text{pu}})] [1/(\tilde{\omega}_{\text{L}} - \omega) - 1/(\tilde{\omega}_{\text{L}}^* - \omega_{\text{pu}})] \quad (21d)$$

$$g_{\text{L}}^3(\omega) = [-1/(\tilde{\omega}_{\text{L}} - \omega)] [1/(\omega - \omega_{\text{pu}})] [1/(\tilde{\omega}_{\text{H}} - \omega) - 1/(\tilde{\omega}_{\text{H}}^* - \omega_{\text{pu}})]. \quad (21e)$$

The first terms in parentheses in (21a)–(21c) have a double-resonance character and describe shifts of the resonances. The second terms in parentheses in (21b)–(21e) describe Raman-type processes.

The most interesting components of $\Delta\chi$ are the off-diagonal ones. They are relevant for two different interesting effects based on linearly and circularly polarised light, respectively.

Using a linearly polarised pump oriented at 45° to a linearly polarised probe beam, the optical Kerr effect becomes proportional to $g_K^3(\omega)$. In the MQW with a sizable HL splitting, $g_K^3(\omega)$ is less resonant than $g_K^1(\omega)$ and $g_K^2(\omega)$, and so the excitonically enhanced Kerr effect is expected to be weak.

The situation changes for a circularly polarised pump beam. Let us consider ‘+’ oriented pump light: $E^{pu} = E_0^{pu}(1, i, 0)$. Then the susceptibility is $\Sigma a_K g_K^1(\omega)$ for a ‘+’ polarised probe and $\Sigma a_K b_K g_K^2(\omega)$ for a ‘-’ polarised probe. The corresponding spectra are shown in figure 5. The relative weights for the two polarisation configurations and the two resonances depend on the detuning and the HL splitting. In the limit of very large detuning, we get the same result as [11, 12]. Our analysis shows that the detuning dependence is obtained by replacing $\rho = \omega_H^{ls}/\omega_L^{ls}$ introduced in [11, 12] by $(\omega_H^{ls} - \omega_{pu})/(\omega_L^{ls} - \omega_{pu})$.

It is straightforward to calculate the polarisation properties of a GaAs bulk crystal. In this case, $\omega_{HL} = 0$, and bulk energies and oscillator strengths should be inserted. This yields

$$\frac{1}{2}g_K^1(\omega) = g_K^2(\omega) = g_K^3(\omega) \quad (22)$$

which is to be inserted in (18a)–(18d). In this case the Kerr effect is of the same magnitude as the phenomena associated with circularly polarised light.

Note that additional effects based on the diagonal elements of $\Delta\chi$ are to be expected, depending on linearly polarised pump and probe oriented parallel or perpendicular, respectively.

5. Conclusions

The dynamical Stark effect in a MQW system exhibits a relatively complex phenomenology with respect to its resonance and polarisation properties. This can of course be expected when dealing with a non-linear optical effect in a system intrinsically and geometrically anisotropic. In the present paper it is shown how the main features of this complexity are accounted for by appropriate density matrix dynamics. As an ordering principle we have used the distinction between Fröhlich-type effects [1, 2] and Mysyrowicz-type effects [3, 4]. Experimentally the former are observed with an infrared pump. Theoretically the Fröhlich type is characterised by the action of the pump field on the exciton wavefunction. After the projection to an exciton basis (5a) and (5b) the Fröhlich-type effect therefore depends on dipole matrix elements \tilde{m}_0, \tilde{m}_1 formed with exciton wavefunctions. The non-resonant effect as reported by Mysyrowicz *et al* [3] and von Lehmen *et al* [4] with a pump in the visible (or very near infrared) arises from the Pauli blocking terms. Therefore the relevant equations (15) contain the electron–electron and the hole–hole submatrices C, D. All dipole moments in equations (15) are of the inter-band type $\tilde{M}_{\varphi\rho}^K$.

Let us finally mention a few points that are left open by the present analysis.

(i) The non-linearities caused by the $\mathbf{E} \cdot \mathbf{r}$ terms in the electron–hole propagation operators (2a) and (2b) should be studied more closely, extending formula (14) to the p

exciton series and the continuum. This may be important for a complete quantitative understanding of the case of infrared pumping and xy polarisation.

(ii) The exchange integrals from [13, 14] should be included in the analysis in order to obtain reliable results for the case of small detuning.

(iii) One should go beyond the approximation assuming a monochromatic pump and study pulsed solutions.

Acknowledgments

We acknowledge useful discussions with R Scholz (Aachen) and the financial support of this project by the Deutsche Forschungsgemeinschaft.

References

- [1] Fröhlich D, Nöthe A and Reimann K 1985 *Phys. Rev. Lett.* **55** 1335
- [2] Fröhlich D, Wille R, Schlapp W and Weimann G 1987 *Phys. Rev. Lett.* **59** 1748
- [3] Mysyrowicz A, Hulin D, Antonetti A, Migus A, Masselink W T and Morkoc H 1986 *Phys. Rev. Lett.* **56** 2748
- [4] von Lehmen A, Chemla D S, Zucker J E and Heritage J P 1986 *Opt. Lett.* **11** 609
- [5] Schmitt-Rink S and Chemla D S 1986 *Phys. Rev. Lett.* **57** 2752
- [6] Balslev I and Stahl A 1988 *Solid State Commun.* **67** 85
- [7] Schmitt-Rink S, Chemla D S and Haug H 1988 *Phys. Rev. B* **37** 941
- [8] Zimmermann R and Hartmann M 1988 *Phys. Status Solidi b* **150** 379
- [9] Schäfer W, Schuldt K-H and Binder R 1988 *Phys. Status Solidi b* **150** 412
- [10] Balslev I, Zimmermann R and Stahl A 1989 *Phys. Rev. B* **40** 4095
- [11] Combescot M 1988 *Solid State Commun.* **68** 471
- [12] Joffre M, Hulin D, Migus A and Combescot M 1989 *Phys. Rev. Lett.* **62** 74
- [13] Stahl A 1988 *Z. Phys. B* **72** 3271
- [14] Schlösser J and Stahl A 1989 *Phys. Status Solidi b* **153** 773
- [15] Lindberg M and Koch S W 1988 *Phys. Rev. B* **38** 3784
- [16] Balslev I and Stahl A 1989 *Proc. NATO ASI series B*, vol 194, ed H Haug and L Banyai (New York: Plenum) pp 159–70
- [17] Zimmermann R 1988 *Phys. Status Solidi b* **146** 545
- [18] Saikan S, Hashimoto N, Kushida T and Namba K 1985 *J. Chem. Phys.* **82** 5409
- [19] Hänsch T and Toschek P 1970 *Z. Phys.* **236** 213
- [20] Wille R 1988 *Thesis* Dortmund, Federal Republic of Germany